Interaction of gold nanotubes with the Si(211) surface: A density functional study

Shyamal Konar,* Monoj Das,† and Bikash C. Gupta‡
Department of Physics, Visva-Bharati, West Bengal 731235, India
(Received 26 May 2010; published 30 September 2010)

We perform first-principles calculations to understand the structural and electrical properties of gold nanotubes supported by Si substrate. The surface of the substrate is chosen to be Si(211) and the gold nanotubes considered here are achiral gold nanotubes with four and five strand rows. Gold nanotubes with four strand rows becomes metallic in nature while the gold nanotubes with five strand rows becomes nonmetallic when they are supported by Si(211). The charge redistribution analysis is done to understand the direction and the amount of charge transfer between the Si(211) and gold nanotube. The direction of charge transfer is further established by calculating the work functions of bare Si(211) and isolated gold nanotubes. In addition, the work function of gold nanotubes supported by Si(211) are calculated and the values are found to be the average of the work function of the bare Si(211) surface and the isolated gold nanotubes.

DOI: 10.1103/PhysRevB.82.125458 PACS number(s): 71.15.Mb, 31.15.A−, 68.43.−h

I. INTRODUCTION

The interesting electrical and mechanical properties of carbon nanotubes (CNTs) (Ref. 1) opened up a new area of research for its application in the field of nanoscience and nanotechnology. It has been proposed/demonstrated that CNTs may be used as sensors, junctions of field effect transistors, microelectrical devices, and as wiring materials for interconnections of either conventional or molecular electronic devices.

The remarkable properties of CNTs and its promising technological applications initiated large number of experimental and theoretical studies for examining the nanotubes of materials other than carbon. For example, gold nanotube (GNT), platinum nanotube (PtNT) and a number of nanotubes of composite materials have been synthesized and their structural and electrical properties have been studied.[2–16] It has been found that the GNT and PtNT have a fascinating ordered structure that resemble with CNT (Refs. 10–13 and 16) and they are metallic in nature. Naturally, like metallic CNTs, the GNTs and PtNTs may be used as wiring material in electronic devices. But for the effective use of the nanotubes (CNT, GNT, and PtNT, etc.) as nanoelectric devices or as interconnects, the nanotubes have to be placed at specific orientation on the technologically important substrates. Recently, with the help of atomic force microscope tip, it has been possible to control the shape of CNT and place them on silicon substrates in an organized way. The stable and specific orientation of nanotube depends on the interaction of the nanotube with the substrate atoms. Some important theoretical studies analyzed the electrical and structural properties of CNTs supported by silicon substrates.[17–22] Based on such studies, experimental studies are in progress for integrating CNTs on bare and modified silicon substrates. Along the same line, GNTs or PtNTs should be supported by the technologically important substrates.

However, we note that there has been no theoretical or experimental study in the direction of placing GNTs on technologically important substrate. A clear understanding of the stability, modification of structural and electronic properties of the GNTs due to their interaction with the Si substrates is of great importance for designing experiments. We, therefore, carry out theoretical study for understanding the structural and electrical properties of GNTs when they are supported by technologically important silicon substrate. Though, GNT(5,3) has been observed experimentally[12,13] but in order to render the calculations tractable and at the same time to have the basic understanding of the interaction of the GNTs with silicon surface, the simple achiral gold nanotubes with four strand rows [GNT(4,4)] and five strand rows [GNT(5,5)] are considered here for adsorption. Again to have a periodic compatibility, we have considered Si(211) surface rather than simple Si(001) surface for GNT adsorption. It must be noted that Si(211) is a stable surface and it is widely used for technological applications.[23–27] The paper is organized as follows: the calculational parameters are given in Sec. II and the results and discussions are presented in Sec. III followed by a summary of our findings in Sec. IV.

II. APPROACH AND METHOD

We have done zero-temperature electronic-structure calculation within the density functional theory to understand the interaction of GNT(4,4) and GNT(5,5) with the Si(211) surface. We have used a slab consisting of seven layers of Si atoms to realize the Si(211) surface and this is shown in the Fig. 1(a). In the Fig. 1(a), the X axis, Y axis, and Z axis correspond to $[\bar{1}11]$, $[01\bar{1}]$, and [211] directions, respectively. The Si(211) surface has three different kinds of Si atoms and they are named as terrace, trench, and edge atoms. The terrace, trench, and edge atoms have two, one, and two dangling bonds each, respectively. The unpassivated silicon atoms in the bottom of the slab are passivated by hydrogen atoms. The electronic structure calculations are performed within 1×4 supercell of Si(211) surface. To have periodic compatibility of GNTs and the Si(211) we have aligned the GNTs in such a way that the tube axis of GNTs coincide with the $[\bar{1}11]$ direction. Furthermore in order to satisfy perfect periodic match between Si(211) surface and GNTs, either the substrate may be squeezed along $[\bar{1}11]$ direction by 1.52–2.16 % or the GNTs may be elongated along the tube axis by

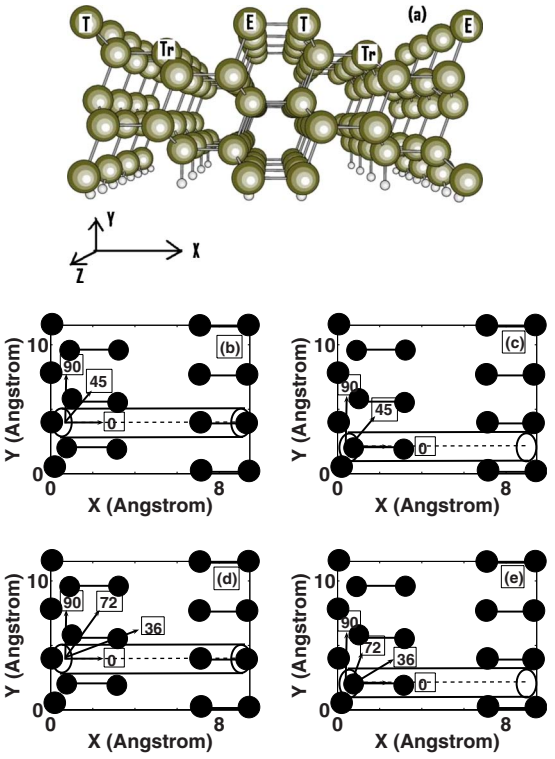

FIG. 1. (Color online) Panel (a) shows the ideal Si(211) surface within 2×4 supercell. The larger filled circles represent the Si atoms and the small unfilled circles represent the hydrogen atoms passivating the bottom most Si atoms. The terrace, trench, and edge atoms are denoted by T, Tr and E, respectively. Panels (b), (c), (d), and (e) shows the schematic diagrams of the T0(4,4), Tr0(4,4), T0(5,5), and Tr0(5,5) geometries. In panels (b)–(d), the larger filled circles denote the top layer Si atoms and smaller filled circles denote Si atoms just below the top layer of the Si(211) surface.

1.55–2.21 %. We found that the electrical and structural properties of elongated GNT and the squeezed Si(211) preserves the main features of the unextended GNT and the uncompressed Si(211) substrate, respectively. Therefore, in this study we have squeezed the Si(211) substrate by 2.16% [for GNT(4,4)] and 1.52% [for GNT(5,5)] along $[\bar{1}11]$ direction to have perfect periodic match between the substrate and the GNT. The expansion of the substrate along $[01\bar{1}]$ and [211] direction is also taken care.

The Si(211) offers two different environments for the adsorption of the GNTs. Either the GNTs may be placed on top of the terrace atoms or on top of the trench atoms along the $[\bar{1}11]$ direction. Furthermore, GNT(4,4) and GNT(5,5) may also rotate about their axis so as to reach the minimum-energy orientation on the Si(211). Since GNT(4,4) and GNT(5,5) has C_4 and C_5 symmetries, respectively, two different initial orientations of the tube are considered at a certain position on the Si(211). The angle of rotation between two orientations of GNT(4,4) and GNT(5,5) are **45**° and **36**°, respectively. All these initial configurations (two positions and two angular orientation about tube axis for each position) takes into account three kinds of motions of the tubes on the Si(211) surface. They are, namely, slipping: lateral movements of nanotube occurs across the surface in a direction perpendicular to its length while no rotation of the GNT occurs, spinning: the nanotube remains in place on surface while the GNT is rotating about its axis and rolling: the nanotube slips and spins simultaneously.

The initial configurations of GNT(4,4) on the Si(211) are denoted as **T**0(4,4), **T45(4,4)** [see Fig. 1(b)], **Tr0(4,4)**, and **Tr45(4,4)** [see Fig. 1(c)] while the initial configurations of GNT(5,5) on the Si(211) are denoted as **T0(5,5)**, **T36(5,5)** [see Fig. 1(d)], **Tr0(5,5)** and **Tr36(5,5)** [see Fig. 1(e)]. The configuration, **T0(4,4)**, corresponds to a situation, where the GNT(4,4) is placed on top of the terrace atoms such that bottom most Au atoms of the tube are just on top of terrace atoms (this is considered as zero rotation). If the tube in the **T0(4,4)** configuration is rotated about its axis by **45**°, we obtain the **T45(4,4)** configuration. Similar conventions are followed for the rest of the configurations. When we consider the adsorption of GNT(4,4) [or GNT(5,5)] on Si(211), the supercell consists of 56 Si atoms, 16 [or 20] Au atoms and 16 H atoms.

First-principles total-energy calculations were carried out within density functional theory at zero temperature using the VASP code.[28–30] The wave functions are expressed by plane waves with the cutoff energy $|k+G|^2 \leq 250$ eV. The Brillouin zone integrations are performed by using the Monkhorst-Pack scheme with $4\times4\times1$ k point meshes for 1×4 primitive cells. Ions are represented by ultrasoft Vanderbilt-type pseudopotentials[31] and results for fully relaxed atomic structures are obtained using the generalized gradient approximation. The preconditioned conjugate gradient method is used for the wave-function optimization and the conjugate gradient method for ionic relaxation. Note that the consecutive slabs are separated by a vacuum space of 40 Å to avoid its interaction with its image.[22,18] The lateral intertube distance along $[01\bar{1}]$ direction is kept $\approx$11 Å to avoid intertube interaction. The Si atoms on the top five silicon layers of the slab are allowed to relax while the lower most silicon layers of the slab and the passivating hydrogen atoms are kept fixed to simulate the bulklike termination. It has been established earlier that the energy cutoff and the set of k points, the number of the layer of the slab and the amount of vacuum region considered here give sufficiently converged values for total-energy calculations. The convergence criteria for energy are taken to be 10^{-5} eV and the systems are relaxed until the force on each atom is below 5.0×10^{-3} eV/Å.

The work function (WF) is calculated by taking the difference between the vacuum level (Φ) and the Fermi-level energy (E_f) (see Fig. 2) and is defined as

$$\mathrm{WF} = \Phi - E_f. \tag{1}$$

The vacuum level Φ is estimated by averaging the electrostatic potential $[V_{av}(z)]$ on a plane at the center of the symmetrical slab along Z axis and can be obtained from Poisson's equation.

$$\frac{\delta^2 V_{av}(z)}{\delta z^2} = -4\pi\rho_{av}(z), \tag{2}$$

where, $\rho_{av}(z)$ is the charge density at z averaged over the xy plane.

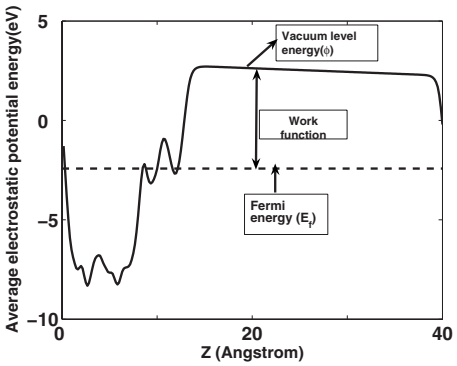

FIG. 2. For the T0(5,5) configuration, the average electrostatic potential in the *X*-*Y* plane is plotted along the *Z*[211] direction.

$$V_{av}(z) = -4\pi\int_{z}^{\infty}\rho_{av}(z')z'dz' + 4\pi z\int_{z}^{\infty}\rho_{av}(z')dz', \quad (3)$$

where

$$\rho_{av}(z) = \frac{\int\int_{A}|\Psi(x,y,z)|^2dxdy}{A}, \quad (4)$$

where, A is the surface area of the unit cell.

III. RESULTS AND DISCUSSIONS

Here we consider two achiral single-wall gold nanotubes, namely, GNT(4,4) and GNT(5,5). These GNT's are first constructed by rolling a two-dimensional Au(111) sheet and then relaxed to obtain the minimum-energy structure. It is found that after complete relaxation, the final atomic structures of GNT(4,4) and GNT(5,5) agree with the structures obtained by Senger *et al.*[13] The description and the results of GNT(4,4) and GNT(5,5) are summarized in the Table I. These relaxed GNTs are then adsorbed on the ideal Si(211) surface as well as on the reconstructed Si(211): 1×2 surface. However, the final atomic structure of the composite system [GNT on Si(211)] is independent of whether the GNT is placed on the ideal Si(211) or on the reconstructed Si(211): 1×2 surface. Therefore, we discuss the energetics of the composite system, where the GNT is initially placed on the ideal Si(211) surface.

To find the most favorable adsorption geometry of a GNT on Si(211) surface, we calculate binding energy of GNT per unit length (E_{BE}) at different adsorption geometries on the surface. The binding energy per unit length of a GNT when adsorbed on the ideal Si(211): 1×1 surface is defined as

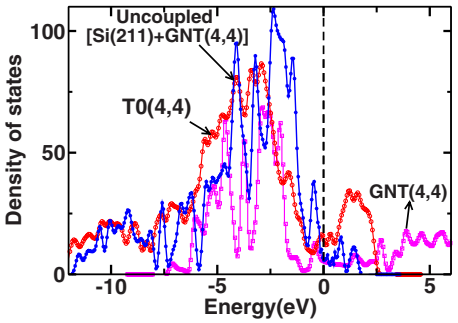

FIG. 3. (Color online) Density of states of isolated GNT(4,4), the GNT(4,4) coupled with Si(211) in the T0(4,4) geometry and that of the uncoupled [Si(211)+GNT(4,4)] system are plotted. Fermi energy level for each case is shifted to 0 eV and shown by dashed line.

$$E_{BE} = \frac{E_{tot}(\mathrm{GNT+Si}) - [E_{tot}(\mathrm{GNT}) + E_{tot}(\mathrm{Si})]}{L}, \quad (5)$$

where, E_{tot}(GNT+Si) corresponds to the total energy of the hybrid structure when GNT is integrated on the ideal Si(211); E_{tot}(GNT) represents the total energy of the isolated GNT; E_{tot}(Si) represents the total energy of the ideal Si(211); and L is the length of the GNT within the 1×4 supercell.

If we consider only slipping of GNT(4,4) on the Si(211) surface with **0**° as initial rotational configuration, the T0(4,4) is the favorable geometry and if the initial rotational configuration is kept at **45**°, the Tr45(4,4) turns out to be the favorable geometry. However, among all these configurations, T0(4,4) is the most favorable configuration.

When the motion of the GNT is constrained to spinning only, T0(4,4) is favorable if the spinning axis of the GNT coincides with the terrace atoms of the surface with E_{BE} =1806 meV/Å and Tr0(4,4) becomes favorable when the spinning axis of the GNT lies on the Trench atoms with E_{BE}=1735 meV/Å. In this case T0(4,4) turns out to be the most stable configuration.

When both the spinning and slipping (i.e., rolling) of the GNT are allowed on the Si(211), the T0(4,4) is the most stable configuration, Tr0(4,4) is the next favorable configuration and the T45(4,4) is the least stable geometry with E_{BE}=1627 meV/Å. This clearly reflects that GNT(4,4) interacts strongly with the Si(211) surface.

To understand the electrical nature of the most favorable configuration of GNT(4,4) on Si(211), the density of states (DOS) of the T0(4,4) configuration is plotted (see Fig. 3) along with the DOS of the isolated GNT(4,4) that of the GNT(4,4) placed 5 Å above the Si(211) surface (this is referred as uncoupled [Si(211)+GNT(4,4)] system). It is clear

TABLE I. Various physical quantities of GNT(4,4) and GNT(5,5) are listed here.

SWGNT	Radius (in Å)	Binding energy per gold atom (in eV)	Length of the unit cell (in Å)	No. of atoms per unit cell	Work function (in eV)
(4,4)	2.04	2.54	4.60	8	5.29
(5,5)	2.44	2.66	4.63	10	5.55

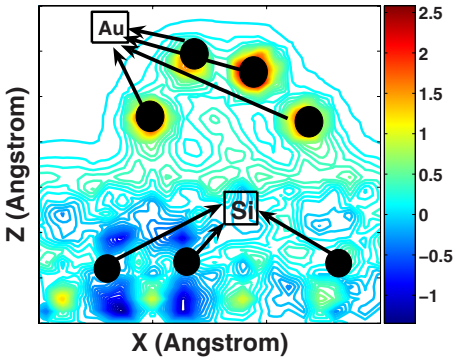

FIG. 4. (Color online) The redistribution of charge density in T0(4,4) geometry is plotted on the plane perpendicular to the $[\bar{1}11]$ direction.

form the Fig. 3 that the DOS increases when the GNT is placed on the Si(211) surface. The increase in the DOS in T0(4,4) geometry near the Fermi energy level (see Fig. 3) confirms the enhancement of the electrical conducting property throughout the contact region due to the interaction of the GNT(4,4) with the Si(211) surface.

To understand the direction of charge transfer between the GNT and the Si(211) for the T0(4,4) configuration, we carry out the charge redistribution analysis. This is done by calculating the total charge-density difference $\Delta\rho$, which is obtained by subtracting the total charge density (TCD) of the isolated GNT(4,4) and that of the isolated Si(211) surface from the total charge density of the composite system. The $\Delta\rho$ is expressed as

$$\Delta\rho = \rho[T0(4,4)] - \rho[\mathrm{Si}(211)] - \rho[\mathrm{GNT}(4,4)], \qquad (6)$$

where $\rho[\mathrm{GNT}(4,4)]$, $\rho[\mathrm{Si}(211)]$, and $\rho[T0(4,4)]$, correspond to the total charge density of the isolated GNT(4,4), of the isolated Si(211) surface and of the composite system, respectively.

The charge-density difference, $\Delta\rho$ plotted in the Fig. 4 shows that some amount of charge has transferred from the Si(211) surface to the GNT(4,4). To estimate the amount of charge transfer from Si(211) to GNT(4,4) in the T0(4,4) configuration, we adopt Bader charge-transfer analysis. The estimated value of total charge gain of GNT(4,4) within the 1×4 supercell is $8.78e$. However, the charge gain by individual gold atoms of the GNT(4,4) ranges from $0.03e$ to $1.89e$. From thermodynamic point of view, in general, charge may transfer from a material of lower work function to a material of higher work function.[32] The results for work function of GNT and Si(211) will be presented in the later part of our discussion and it can be seen that the work function of Si(211) is smaller than the GNT(4,4). Thus, the charge transfer from Si surface to the GNT(4,4) is reasonable.

The relaxed atomic structure of the composite system in the T0(4,4) configuration is shown in the Fig. 5. In this structure, the Au-Si bond lengths range from 2.42 to 2.68 Å, the Au-Au bond lengths range from 2.50 to 2.89 Å and the contact area between the GNT(4,4) and Si(211) surface within the 1×4 supercell is $\approx$71.94 Å^2. From the relaxed atomic

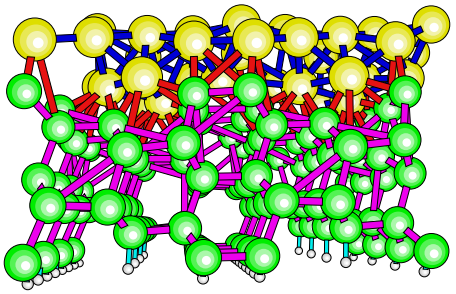

FIG. 5. (Color online) Relaxed atomic structure of GNT(4,4) supported by Si(211) surface in T0(4,4) geometry is shown. The larger spheres represent the Au atoms, the relatively smaller spheres represent the Si atoms and the smallest spheres at the bottom represent the H atoms.

structure it is visible that the GNT(4,4) is deformed to a large extent. To understand the degree of deformation, we define the deformation ratio (ΔD) as

$$\Delta D = \frac{D_{\max} - D_{\min}}{\bar{D}}, \qquad (7)$$

where $D_{\max}$, $D_{\min}$, and $\bar{D}$ are the maximum diameter, the minimum diameter and the average diameter of the GNT, respectively, after the complete relaxation of the hybrid system. The calculated value of the deformation ratio of GNT(4,4) in T0(4,4) geometry is 64%. This large deformation indicates that GNT(4,4) experiences a large shearing force due to strong Au-Si interaction. In spite of large deformation of the GNT in the T0(4,4) configuration, the hollowness of the tube on the Si(211) is retained and this is clear from the total charge-density plot in a plane perpendicular to the tube axis (see Fig. 6).

Here, we consider the second most favorable configuration, Tr0(4,4), to discuss the structural and electrical properties of the relaxed composite structure. The relaxed atomic structure in this configuration reveals that the GNT on the Si(211) is highly deformed in comparison to its ideal structure due to the strong interaction of the GNT(4,4) with the Si(211) surface. However, the total charge density on a plane perpendicular to the axis of the GNT shows that the

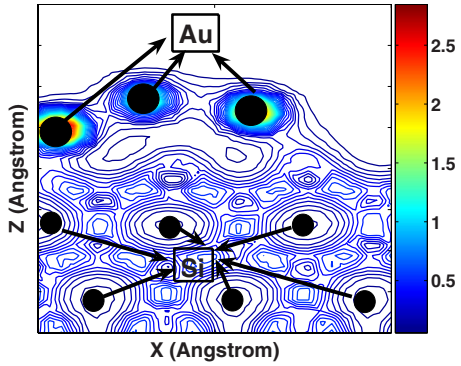

FIG. 6. (Color online) TCD of GNT(4,4) supported by Si(211) surface in T0(4,4) geometry is plotted on the plane perpendicular to the $[\bar{1}11]$ direction.

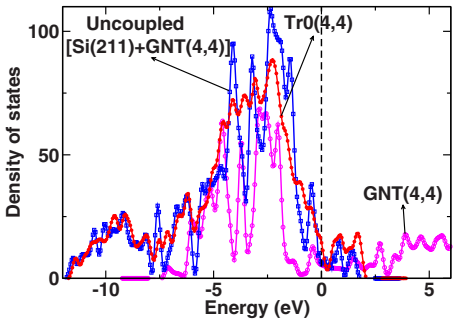

FIG. 7. (Color online) Density of states of isolated GNT(4,4), the GNT(4,4) coupled with Si(211) in the Tr0(4,4) geometry and that of the uncoupled [Si(211)+GNT(4,4)] system are plotted. Fermi energy level for each case is shifted to 0 eV and shown by dashed line.

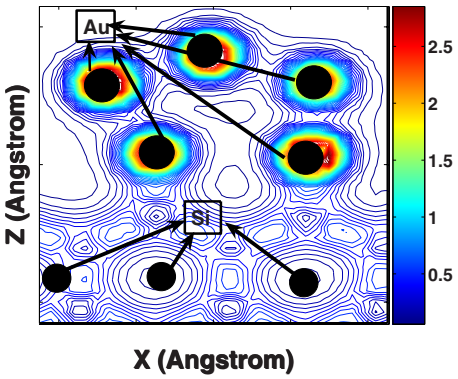

FIG. 8. (Color online) TCD in T0(5,5) geometry is plotted on the plane perpendicular to the $[\bar{1}11]$ direction.

GNT(4,4) on the Si(211) retains the hollowness of the tube. The Si-Au bond lengths and Au-Au bond length in this case ranges from 2.40 to 2.44 Å and 2.74 to 2.84 Å, respectively.

To understand the electrical properties of GNT(4,4) on Si(211) in the Tr0(4,4) configuration, we have plotted the DOS of the isolated GNT(4,4), the uncoupled [Si(211)+GNT(4,4)] and that of the Tr0(4,4) configuration (see Fig. 7). From the Fig. 7, we find that in the Tr0(4,4) configuration, the density of states around the Fermi energy level increases due to the interaction of the GNT(4,4) with the Si(211) surface and hence we may conclude that the metallicity of the GNT(4,4) on the Si(211) increases.

In the process of integration of GNT(5,5) on Si(211) surface, T0(5,5) is the most stable geometry with E_{BE}1680 eV/Å and T36(5,5) is the least stable geometry with E_{BE}1386 eV/Å (see Table. II). The Si-Au and Au-Au bond lengths for the most stable configuration, T0(5,5), ranges from 2.38 to 2.51 Å and 2.73 to 2.91 Å, respectively. The TCD in T0(5,5) geometry on a plane perpendicular to the $[\bar{1}11]$ direction (see in Fig. 8) reveals that the tubular structure is remain intact after the complete relaxation. Density of states of the isolated GNT(5,5), that of GNT(5,5) on Si(211) in the T0(5,5) geometry and that of the uncoupled [Si(211)+GNT(5,5)] system are plotted in Fig. 9. The density of states near the Fermi energy level reveals that the GNT(5,5) becomes nonmetallic when it is supported on Si(211) surface.

For the completeness of our discussions on the charge transfer from Si(211) surface to GNT, the values of the work functions of bare Si(211) surface, the isolated GNTs are mandatory. Our calculations reveal that the work functions of GNT(4,4), GNT(5,5) and Si(211) surface are ~5.29 eV, ~5.55 eV, (see Table. I) and ~4.79 eV, respectively. It is clear that the work functions of GNT(44) and GNT(5,5) are larger than Si(211) surface by 0.5 eV and 0.76 eV, respectively, which in turn support the direction of charge transfer from Si(211) to the GNTs.

As the work function is an important quantity for determining various electrical properties, we have also estimated the work function of the hybrid system [GNTs on Si(211)] and displayed in the Table II. We find that the work function of the composite system depends on the orientation of the GNTs on the Si(211) surface. However, for the most stable configurations, the work function of the composite systems lies around 5 eV which is roughly the average of the work functions of the bare Si(211) and that of an isolated GNT.

It may be noticed that among all the possible geometries of the GNT(4,4) on the Si(211) surface, the relaxed T0(4,4) is the most stable configuration and in this configuration the metallicity of the GNT(4,4) is enhanced. Therefore, GNT placed on Si(211) may play an important role as metallic interconnects in circuit devices. Furthermore, the GNTs on Si(211) may be technologically important for the development of nanoscale devices. We, therefore conclude that experiments may be designed in this direction to realize the GNTs supported by Si substrates.

TABLE II. BE (in meV/Å) and work function (in eV) of the hybrid structure are tabled. The distributions of (Si-Au) and (Au-Au) bond lengths are also tabled.

Configurations	E_{BE}(GNT) (in meV/Å)	Work function (in eV)	Si-Au bond length (in Å)	Au-Au bond length (in Å)
T0(4,4)	1806	5.01	2.42–2.68	2.50–2.89
T45(4,4)	1627	4.92	2.34–2.41	2.78–2.98
Tr0(4,4)	1735	5.04	2.40–2.44	2.74–2.84
Tr45(4,4)	1692	4.93	2.37–2.55	2.83–2.98
T0(5,5)	1680	5.16	2.38–2.51	2.73–2.91
T36(5,5)	1386	4.95	2.43–2.70	2.67–2.92
Tr0(5,5)	1652	3.51	2.36–2.39	2.74–3.01

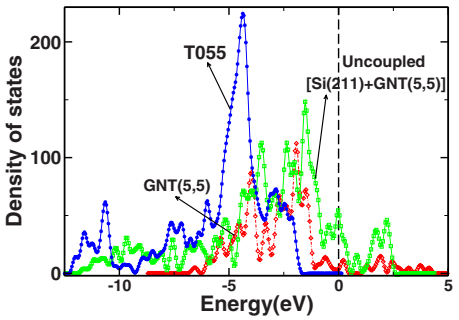

FIG. 9. (Color online) Density of states of isolated GNT(5,5), the GNT(5,5) coupled with Si(211) in the T0(5,5) geometry and that of the uncoupled [Si(211)+GNT(5,5)] system are plotted. Fermi energy level for each case is shifted to 0 eV and shown by dashed line.

IV. SUMMARY

We have performed the density functional calculations to understand the electronic an structural properties of GNTs supported by Si(211) surface. We found that GNT(4,4) interacts strongly with the Si(211) and the most stable configuration of GNT(4,4) on Si(211) is metallic in nature. However, the most stable configuration of GNT(5,5) on Si(211) turns out to be nonmetallic in nature. In addition, we have done the charge redistribution analysis to understand the direction of charge transfer and employed the bader analysis to estimate the amount of charge transfer from Si(211) to the GNT(4,4). An important quantity, namely, the work function is calculated for the bare Si(211), isolated GNTs and for the composite system comprising of GNT and Si(211).

ACKNOWLEDGMENTS

One of the authors, B.C.G. acknowledges the partial financial support from the CSIR funded under Project No. 03(1081)/06/EMR-II, India. Also B.C.G. would like to thank University of Illinois at Chicago for hospitality during the work.

*shyam_konar@yahoo.co.in
†dsmonoj@gmail.com
‡bikash@uic.edu

[1] S. Iijima, Nature (London) **354**, 56 (1991); T. Ichihasi, *ibid.* **363**, 603 (1993).
[2] J. Sha, J. Niu, X. Ma, J. Xu, X. Zhang, Q. Yang, and D. Yang, Adv. Mater. **14**, 1219 (2002).
[3] J. Cumings and A. Zettl, Chem. Phys. Lett. **316**, 211 (2000).
[4] Q. Wu, Z. Hu, X. Wang, Y. Lu, X. Chen, H. Xu, and Y. Chen, J. Am. Chem. Soc. **125**, 10176 (2003).
[5] J. Goldberger, R. He, Y. Zhang, S. Lee, H. Yan, H.-J. Choi, and P. Yang, Nature (London) **422**, 599 (2003).
[6] X. H. Sun, C. Li, W. K. Wong, N. B. Wong, C. S. Lee, S. T. Lee, and B. K. Teo, J. Am. Chem. Soc. **124**, 14464 (2002).
[7] M. Menon, E. Richter, A. Mavrandonakis, G. Froudakis, and A. N. Andriotis, Phys. Rev. B **69**, 115322 (2004).
[8] K. M. Alam and A. K. Ray, Nanotechnology **18**, 495706 (2007).
[9] K. M. Alam and A. K. Ray, Phys. Rev. B **77**, 035436 (2008).
[10] Y. Kondo and K. Takayanagi, Science **289**, 606 (2000).
[11] Y. Oshima, A. Onga, and K. Takayanagi, Phys. Rev. Lett. **91**, 205503 (2003).
[12] Y. Oshima, H. Koizumi, K. Mouri, H. Hirayama, K. Takayanagi, and Y. Kondo, Phys. Rev. B **65**, 121401(R) (2002).
[13] R. T. Senger, S. Dag, and S. Ciraci, Phys. Rev. Lett. **93**, 196807 (2004).
[14] C. K. Yang, Appl. Phys. Lett. **85**, 2923 (2004).
[15] S. L. Elizondo and J. W. Mintmire, Phys. Rev. B **73**, 045431 (2006).
[16] S. Konar and B. C. Gupta, Phys. Rev. B **78**, 235414 (2008).
[17] K. Kamaras, M. E. Itkis, H. Hu, B. Zhao, and R. C. Haddon, Science **301**, 1501 (2003).
[18] W. Orellana, R. H. Miwa, and A. Fazzio, Phys. Rev. Lett. **91**, 166802 (2003).
[19] Y. H. Kim, M. J. Heben, and S. B. Zhang, Phys. Rev. Lett. **92**, 176102 (2004).
[20] P. M. Albrecht and J. W. Lyding, Nanotechnology **18**, 125302 (2007).
[21] P. M. Albrecht, S. B. Lopez, and J. W. Lyding, Nanotechnology **18**, 095204 (2007).
[22] R. H. Miwa, W. Orellana, and A. Fazzio, Appl. Phys. Lett. **86**, 213111 (2005).
[23] D. J. Chadi, Phys. Rev. B **29**, 785 (1984).
[24] R. Kaplan, Surf. Sci. **116**, 104 (1982).
[25] J. E. Yater, A. Shih, and Y. U. Idzerda, Phys. Rev. B **51**, 7365 (1995).
[26] O. J. Glembocki and S. M. Prokes, Appl. Phys. Lett. **71**, 2355 (1997).
[27] A. A. Baski, S. C. Erwin, and L. J. Whitman, Surf. Sci. Lett. **423**, L265 (1999).
[28] G. Kresse and J. Hafner, Phys. Rev. B **47**, 558 (1993); **49**, 14251 (1994).
[29] G. Kresse and J. Furthmüller, Comput. Mater. Sci. **6**, 15 (1996).
[30] G. Kresse and J. Furthmüller, Phys. Rev. B **54**, 11169 (1996).
[31] G. Kresse, and J. Hafner, J. Phys.: Condens. Matter **B6**, 8245 (1994).
[32] S. J. Sque, R. Jones, S. Öberg, and P. R. Briddon, Phys. Rev. B **75**, 115328 (2007).